Journal of Alloys and Compounds 509 (2011) 4958–4966

Contents lists available at ScienceDirect

Journal of Alloys and Compounds

journal homepage: www.elsevier.com/locate/jallcom

Solid-state reactive diffusion between Ni and W

S. Inomata [a], M. Kajihara [b,*]

[a] Graduate School, Tokyo Institute of Technology, Yokohama 226-8502, Japan
[b] Department of Materials Science and Engineering, Tokyo Institute of Technology, Nagatsuta 4259-J2-59, Midori-ku, Yokohama 226-8502, Japan

ARTICLE INFO

Article history:
Received 10 August 2010
Accepted 23 January 2011
Available online 2 February 2011

Keywords:
Intermetallics
Grain boundaries
Kinetics
Modeling

ABSTRACT

Various alloys are interconnected with W using a Ni intermediate layer by the diffusion bonding (DB) technique. During solid-state heating in the DB technique, however, reactive diffusion occurs at the interconnection between Ni and W. In order to examine the kinetics of the reactive diffusion, sandwich Ni/W/Ni diffusion couples were isothermally annealed at temperatures of T = 1023–1173 K for various times up to t = 366 h. Owing to annealing, Ni_4W is produced as a layer at the Ni/W interface in the diffusion couple and grows predominantly towards Ni. The thickness of the Ni_4W layer increases in proportion to a power function of the annealing time. The exponent of the power function is close to 0.5 at T = 1173 K and gradually decreases with decreasing annealing temperature. Furthermore, grain growth takes place in Ni_4W due to annealing. Therefore, volume diffusion is the rate-controlling process for the growth of Ni_4W at T = 1173 K. At T < 1173 K, however, boundary diffusion contributes to the rate-controlling process, and the contribution of boundary diffusion increases with decreasing annealing temperature. On the other hand, a region alloyed with W is formed in Ni from the Ni_4W/Ni interface by diffusion-induced recrystallization (DIR). The growth rate of the DIR region is much greater than the penetration rate of W into Ni by volume diffusion, and the concentration of W in the DIR region at the Ni_4W/Ni interface is equal to the solubility of W in Ni. Such growth behavior of the DIR region was numerically analyzed using a mathematical model. The analysis indicates that the growth of the DIR region is controlled by the interface reaction at the moving boundary of the DIR region as well as the boundary diffusion along the grain boundaries across the DIR region under the present annealing conditions.

1. Introduction

The diffusion bonding (DB) technique realizes interconnection between similar and dissimilar materials without melting. As a result, unlike welding, brazing and soldering, this technique is able to prevent microstructural defects produced by solidification of molten materials. Hence, the DB technique is widely used in various manufacturing processes. The interconnection between W and different alloys has been studied using the DB technique by many investigators [1–4]. In order to improve adherence of the interconnection, a Ni intermediate layer is usually inserted into the interconnection. The melting temperature is 1728 K and 3695 K for Ni and W, respectively [5], but the bonding temperature is typically around 1000 K. Hence, the bonding temperature is much lower than the melting temperature. Nevertheless, during diffusion bonding, solid-state reactive diffusion rather quickly occurs at the Ni/W interface of the interconnection. Such reactive diffusion yields microstructure evolution and hence will influence the mechanical properties of the interconnection. Therefore, kinetic information on the reactive diffusion is essentially important to actualize sound interconnection by the DB technique.

The reactive diffusion between Ni and W was experimentally observed by Xu et al. [1] In this experiment, W/Ni/$Si_{0.8}Ge_{0.2}$ diffusion couples were isothermally annealed at temperatures between T = 1053 K and 1173 K for various times up to t = 4 h. According to their observation, a Ni_4W layer is formed at the Ni/W interface in the diffusion couple due to annealing. Under their annealing conditions, however, the thickness of the Ni_4W layer is not large enough to determine reliably the chemical composition by energy dispersive spectrometry (EDS). A similar experiment was conducted by Zhong et al. [3] In their experiment, isothermal annealing of W/Ni/(Fe–17Cr) diffusion couples was carried out at a temperature of T = 1173 K for various periods between t = 0.5 h and 2 h. At the Ni/W interface in the annealed diffusion couple, the Ni_4W layer was observed for t = 2 h but not for t = 0.5–1.5 h. This implies that there exists an incubation period for formation of Ni_4W. According to a recent phase diagram in the binary Ni–W system [5], NiW and NiW_2 as well as Ni_4W appear as stable intermetallic compounds at T = 1173 K. However, NiW and NiW_2 were not recognized in the experiment by Zhong et al. [3] On the other hand, their experimental result indicates that the penetration of W into Ni from the Ni/W interface continuously occurs during annealing and the

* Corresponding author. Tel.: +81 45 924 5635; fax: +81 45 924 5857.
E-mail address: kajihara@materia.titech.ac.jp (M. Kajihara).

0925-8388/$ – see front matter © 2011 Elsevier B.V. All rights reserved.
doi:10.1016/j.jallcom.2011.01.139

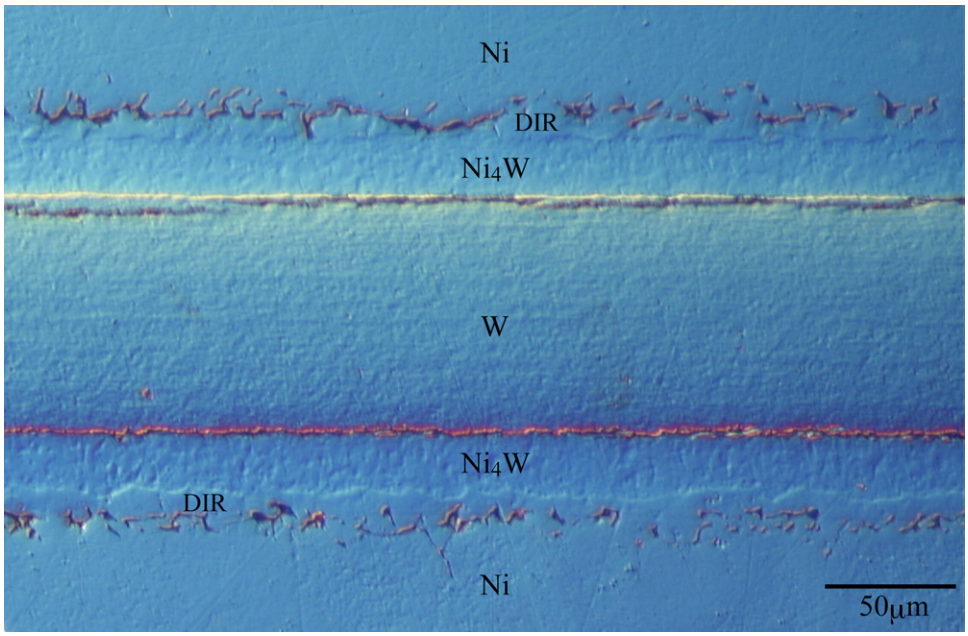

Fig. 1. OM photograph of cross-section normal to the parallel interfaces of the Ni/W/Ni diffusion couple annealed at 1123 K for 186 h (670 ks).

penetration distance d reaches to 5 μm for t = 1.5 h at T = 1173 K. If the penetration is controlled by volume diffusion, d is roughly estimated by the parabolic relationship $d = 2\sqrt{Dt}$. Here, D is the diffusion coefficient for volume diffusion of W in Ni. Using a value of $D = 9.2 \times 10^{-18}$ m^2/s at T = 1173 K [6], we obtain d = 0.45 μm for t = 1.5 h from the parabolic relationship. Hence, d is one order of magnitude greater for the experiment than for the estimation. This means that the penetration is governed by shortcut diffusion. Nevertheless, such shortcut diffusion was not mentioned in most of the studies. The fast penetration of W into Ni as well as the formation of Ni_4W may affect the mechanical properties of the interconnection. Unfortunately, however, no reliable kinetic information is available not only for the fast W diffusion into Ni but also for the Ni_4W growth. In order to obtain such kinetic information, the solid-state reactive diffusion between Ni and W was experimentally examined using sandwich Ni/W/Ni diffusion couples in the present study. The diffusion couple was isothermally annealed in the temperature range of T = 1023–1173 K, and then the microstructure evolution in the diffusion couple was observed in a metallographical manner. The observation was numerically analyzed using mathematical models.

2. Experimental

Polycrystalline specimens with a dimension of 12 mm × 5 mm × 1 mm were cut from a commercial plate of pure Ni with a thickness of 1 mm and purity higher than 99.7%. The Ni plate specimens were separately annealed in evacuated silica capsules at 1473 K for 1 h. The two surfaces with an area of 12 mm × 5 mm of each annealed Ni plate specimen were mechanically polished on 400–4000 emery papers until a depth of 100 μm and then finished using diamond with a diameter of 1 μm. After mechanical polishing and finishing, the pure Ni plate specimen was electrolytically polished with a cathode of Ag in an etchant consisting of 5 vol.% of sulfuric acid and 95 vol.% of distilled water at voltages of 3.5–5 V for 30 s at 273 K.

Pure W sheet specimens with a dimension of 12 mm × 5 mm × 0.1 mm were cut from a commercial sheet with a thickness of 0.1 mm and purity higher than 99.95% and then degreased in acetone with an ultrasonic cleaner. After degreasing, each W sheet specimen was immediately sandwiched between the finished surfaces of two freshly prepared Ni plate specimens in ethanol by the technique reported in a previous study [7]. Each sandwich couple was completely dried and then isothermally heat-treated for diffusion bonding in an evacuated silica tube, followed by air-cooling. The diffusion bonding was carried out at temperatures of 1023 K, 1073 K, 1123 K and 1173 K for times of 113 h, 113 h, 112 h and 75 h, respectively. The diffusion couples were separately encapsulated in evacuated silica capsules and then isothermally annealed at temperatures of 1023 K, 1073 K, 1123 K and 1173 K for various times up to 253 h, followed by water-quenching without breaking the capsules. Hereafter, the summation of the heat-treating and annealing times is merely called the annealing time t, and the annealing temperature is denoted by T. Cross-sections of the annealed diffusion couple were mechanically polished using 1000–4000 emery papers and diamond with a size of 1 μm and then finished with an OP-S liquid manufactured by Struers Ltd. The microstructure of the cross-section was observed by optical microscopy (OM). Concentration profiles of Ni and W on the cross-section were measured by electron probe microanalysis (EPMA).

3. Results and discussion

3.1. Microstructure

A typical OM photograph for the cross-section of the annealed diffusion couple is shown in Fig. 1. This figure indicates the photograph for the diffusion couple with an annealing temperature of T = 1123 K and an annealing time of t = 186 h (670 ks). In Fig. 1, the upper-side and lower-side regions are the Ni plate specimens, and the horizontal band with a thickness of about 100 μm is the W sheet specimen. As can be seen, a polycrystalline layer with a thickness of about 20 μm is formed between the W and Ni specimens. Concentration profiles of Ni and W across the polycrystalline layer were measured by EPMA. A typical result of the diffusion couple with T = 1023 K and t = 209.95 h (756 ks) is shown as open circles in Fig. 2. In this figure, the ordinate and the abscissa indicate the mol fraction y of W and the distance x, respectively. The EPMA measurement in Fig. 2 shows that the polycrystalline layer between the W and Ni specimens is Ni_4W. The Ni_4W layer was recognized in all the diffusion couples annealed at T = 1023–1173 K. Since W is brittle, cracks are sometimes formed in the W specimen along directions almost parallel to the W/Ni_4W interface during mechanical polishing as shown in Fig. 1. The crack direction may be relevant to the initial microstructure of the commercial W sheet.

According to a recent phase diagram in the binary Ni–W system [5], Ni_4W, NiW and NiW_2 are the stable intermetallic compounds at T = 1023–1173 K. However, NiW and NiW_2 were not recognized in the present study. As mentioned in Section 1, such an observation was reported also by Zhong et al. [3,4] On the other hand, the solid-state reactive diffusion between Au and Sn was experimentally examined in previous studies [8–11]. In these experiments, sand-

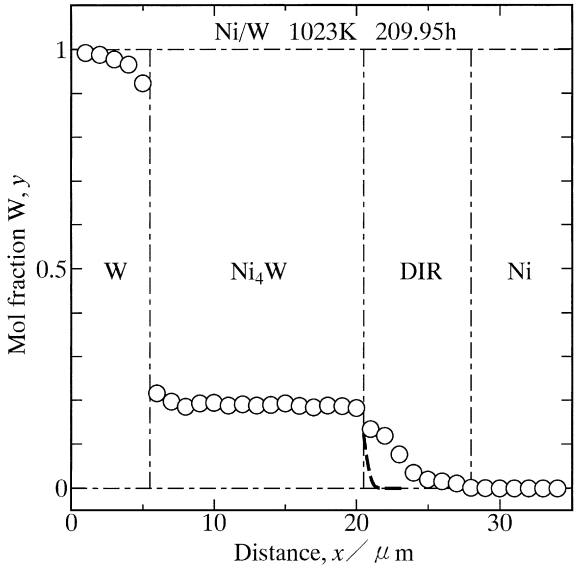

Fig. 2. Concentration profile of W across the Ni_4W layer and the DIR region in the Ni/W/Ni diffusion couple annealed at 1023 K for 209.95 h (756 ks). Open circles show the EPMA measurement, and a dashed curve indicates the calculation from Eq. (1).

wich Sn/Au/Sn diffusion couples were isothermally annealed at temperatures of T = 393–473 K. Owing to annealing, compound layers of $AuSn_4$, $AuSn_2$ and AuSn are produced at the Au/Sn interface in the diffusion couple. However, stable Au_5Sn and ζ compounds [12] were not observed clearly. According to the kinetic analysis of reactive diffusion in a previous study [13], the growth rate of a compound layer is sensitive to the interdiffusion coefficient of the growing compound. If the interdiffusion coefficient is much smaller for a compound layer than for the neighboring phases in a semi-infinite diffusion couple, the compound layer cannot grow up to visible thicknesses within realistic annealing times [13]. This is the case for the Au_5Sn and ζ compounds in the solid-state reactive diffusion between Au and Sn [8–11]. If NiW and NiW_2 are actually stable at T = 1023–1173 K [5], the observation in the present study and that by Zhong et al. [3,4] imply that the interdiffusion coefficient is much smaller for NiW and NiW_2 than for Ni_4W.

Like many other investigations [1–4], the solid-state reactive diffusion between Ni and W was experimentally studied by Walsh and Donachie [14]. In this experiment, Ni/W diffusion couples were isothermally annealed at T = 1273 K for t = 100 h and at T = 1311 K for t = 112–600 h. A similar experiment was conducted at T = 1073–1423 K by Poulsen et al. [15] According to the result by Walsh and Donachie [14], only NiW was observed in the annealed diffusion couples. In contrast, Poulsen et al. [15] reported that Ni_4W, NiW and NiW_2 were formed by annealing at T = 1073–1273 K, T = 1073–1363 K and T = 1073–1313 K, respectively. Consequently, there exists contradiction among the results reported by the different research groups [3,4,14,15]. Recently, the existence of NiW and NiW_2 in the binary Ni–W system was critically discussed by Cury et al. [16] They insist that a small amount of C in Ni–W alloys enhances the formation of Ni_6W_6C and Ni_2W_4C and thus NiW and NiW_2 observed in the Ni/W diffusion couples [14,15] may be Ni_6W_6C and Ni_2W_4C, respectively. If C is practically an impurity of the Ni/W diffusion couple [14,15], their insistence is valid. Unfortunately, however, the concentration of C in the Ni/W diffusion couple was not determined by Walsh and Donachie [14] and by Poulsen et al. [15] In order to judge conclusively the phase stabilities of NiW and NiW_2, however, more reliable information on the phase equilibria in the binary Ni–W system is necessary.

Although the grain boundary in the Ni specimen is not clearly observable in Fig. 1, the mean grain size of the Ni specimen becomes greater than 80 μm after annealing at 1473 K for 1 h. As can be seen in Fig. 1, however, fine grains with sizes smaller than 20 μm are recognized between the Ni_4W layer and the Ni specimen. This fine grain region is produced by diffusion-induced recrystallization (DIR). Here, DIR is the phenomenon that new fine grains with discontinuously different solute concentrations are formed behind moving grain boundaries owing to recrystallization combined with diffusion of solute atoms along the moving and stationary boundaries surrounding the fine grains [17–19]. This fine grain region produced by DIR is hereafter called the DIR region. Furthermore, small Kirkendall voids are observed at the grain boundary between the DIR region and the untransformed matrix of the Ni specimen, and the grain size is slightly greater for the DIR region than for the Ni_4W layer. Hence, the grain boundary between the untransformed matrix and the DIR region as well as the interface between the Ni_4W layer and the DIR region is recognizable in the OM photographs without chemical etching like Fig. 1. As the annealing time increases, the thickness gradually increases for the Ni_4W layer and the DIR region but merely slightly decreases for the W specimen. This means that both the Ni_4W layer and the DIR region grow mainly towards the Ni specimen but hardly into the W specimen. Thus, the migration rate is greater for the grain boundary between the untransformed matrix and the DIR region than for the interface between the Ni_4W layer and the DIR region. Therefore, for convenience' sake, the former grain boundary is called the moving boundary, but the latter interface is designated the stationary interface.

If the interdiffusion coefficient D and the molar volume V_m are both constant and independent of composition at a constant temperature, y is expressed as an explicit function of x and t at $x > x_0$ by the following equation for the penetration of W into the Ni specimen due to volume diffusion [20]:

$$y = y_i - (y_i - y_0)\,\mathrm{erf}\left(\frac{x - x_0}{2\sqrt{Dt}}\right). \quad (1)$$

Here, x_0 is the position of the stationary interface, y_0 is the initial mol fraction of W in the Ni specimen, and y_i is the mol fraction of W in the Ni specimen at the stationary interface. For the Ni/W/Ni diffusion couple, $y_0 = 0$. Although D is considered independent of y, D may vary depending on y. The dependence of D on y at T = 1173–1573 K was experimentally examined by Karunaratne et al. [21]. According to their result, D is insensitive to y. Therefore, D is actually almost independent of y and hence close to the tracer diffusion coefficient D^*_W of W in Ni [22,23]. The temperature dependence of D^*_W is described by the equation

$$D^*_W = D^*_{W0}\ \exp\left(-\frac{Q}{RT}\right), \quad (2)$$

where D^*_{W0} and Q are the pre-exponential factor and the activation enthalpy, respectively. The following values are reported for $D^*_W : D^*_{W0} = 1.9 \times 10^{-4}$ m^2/s and Q = 299 kJ/mol [6]. Using these parameters, y was calculated as a function of x at T = 1023 K for t = 209.95 h (756 ks). The result is shown as a dashed curve in Fig. 2. As can be seen, the thickness of the DIR region is mostly one order of magnitude greater than the penetration depth of the volume diffusion. Consequently, alloying of Ni with W occurs fast due to DIR under the present annealing conditions. Furthermore, the EPMA measurement indicates that y_i is equal to the solubility of W in Ni [5] at each annealing temperature. This means that the local equilibrium is realized at the stationary interface between the DIR region and the Ni_4W layer.

3.2. Growth behavior of Ni_4W

As mentioned in Section 3.1, the Ni_4W layer is produced in the diffusion couple at T = 1023–1173 K. From the OM photographs of the cross-section like Fig. 1, the mean thickness z of the Ni_4W layer

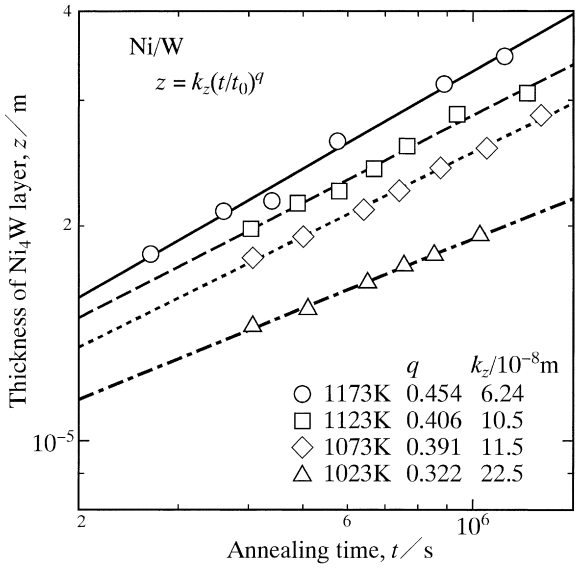

Fig. 3. The thickness z of the Ni_4W layer versus the annealing time t shown as open triangles, rhombuses, squares and circles at 1023 K, 1073 K, 1123 K and 1173 K, respectively. Straight lines indicate the calculations from Eq. (4).

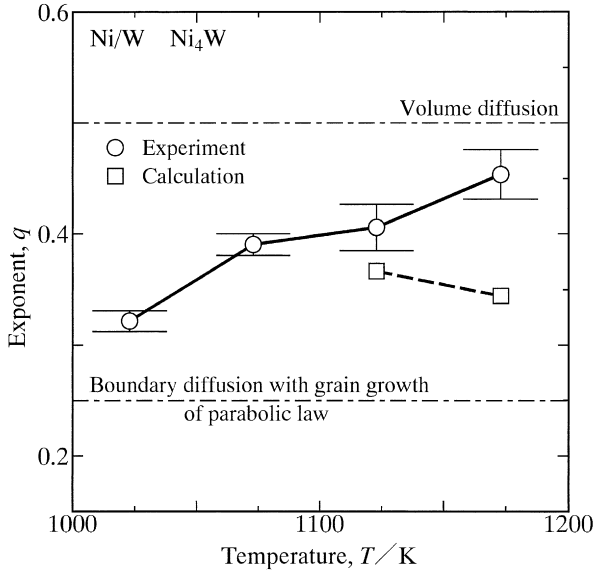

Fig. 4. The exponent q versus the annealing temperature T for the thickness z of the Ni_4W layer shown as open circles with error bars. The calculations with T = 1123–1173 K from Eq. (9) for the result in Fig. 5 are indicated as open squares.

was evaluated at each annealing time by the equation

$$z = \frac{A}{w}, \tag{3}$$

where A is the total area of the Ni_4W layer and w is the total length of the Ni_4W layer parallel to the W/Ni_4W interface. The results of T = 1023 K, 1073 K, 1123 K and 1173 K are plotted as open triangles, rhombuses, squares and circles, respectively, in Fig. 3. In this figure, the ordinate and the abscissa show the logarithms of z and t, respectively. As can be seen, the thickness z monotonically increases with increasing annealing time t. Furthermore, the plotted points for each annealing temperature are located well on a straight line. This means that z is mathematically expressed as a power function of t as follows.

$$z = k_z\left(\frac{t}{t_0}\right)^q \tag{4}$$

Here, t_0 is unit time, 1 s. It is adopted to make the argument t/t_0 of the power function dimensionless. The proportionality coefficient k_z has the same dimension as the thickness z, and the exponent q is dimensionless. From the plotted points in Fig. 3, k_z and q were determined by the least-squares method as indicated with dashed-and-dotted, dotted, dashed and solid lines for T = 1023 K, 1073 K, 1123 K and 1173 K, respectively.

The exponent q is plotted against the annealing temperature T as open circles with error bars in Fig. 4. As can be seen, q is slightly smaller than but rather close to 0.5 at T = 1173 K. On the other hand, q monotonically decreases with decreasing annealing temperature T and becomes much smaller than 0.5 at T = 1023 K. If the growth of the Ni_4W layer is controlled by volume diffusion, q is equal to 0.5 [13,24–27]. On the other hand, boundary diffusion may govern the layer growth at low temperatures where volume diffusion is frozen out. When the layer growth is purely controlled by boundary diffusion across the Ni_4W layer and grain growth occurs in the Ni_4W layer, q is smaller than 0.5 [28]. However, q becomes equal to 0.5 even for the layer growth controlled by boundary diffusion unless grain growth takes place [28]. Consequently, in the case of q = 0.5, there are two possibilities for the rate-controlling process. In such a case, the rate-controlling process cannot be conclusively determined only from the value of q. In order to estimate the rate-controlling process for the layer growth, the grain growth in the Ni_4W layer should be observed experimentally.

As shown in Fig. 1, the Ni_4W layer consists of columnar grains. The mean size u of the columnar grain on the cross-section was evaluated by the equation

$$u = \frac{w}{m}, \tag{5}$$

where m is the number of the columnar grains intersected by a test line of the length w parallel to the W/Ni_4W interface. Assuming that the rotation axis of the columnar grain with a constant diameter d is perpendicular to the interface and parallel to the cross-section, we obtain the equation [29]

$$ud = \pi\left(\frac{d}{2}\right)^2 \tag{6}$$

and hence the relationship [29]

$$d = \frac{4u}{\pi}. \tag{7}$$

From Eq. (7), the mean size u on the cross-section is converted into the diameter or grain size d. The results of T = 1123 K and 1173 K are shown as open squares and circles, respectively, in Fig. 5. At T = 1023 K and 1073 K, however, u was very small and thus could not be reliably determined by the OM observation. In Fig. 5, the ordinate and the abscissa indicate the logarithms of d and t, respectively. As can be seen, the grain size d monotonically increases with increasing annealing time t. Hence, grain growth surely occurs in the Ni_4W layer. Furthermore, the plotted points for each annealing temperature lie well on a straight line. As a consequence, d is mathematically expressed as a power function of t by the following equation of the same formula as Eq. (4).

$$d = k_d\left(\frac{t}{t_0}\right)^p \tag{8}$$

From the plotted points in Fig. 5, the proportionality coefficient k_d and the exponent p were determined by the least-squares method. The determined values of k_d and p yield dashed and solid lines for T = 1123 K and 1173 K, respectively, in Fig. 5. If the growth of the Ni_4W layer is purely controlled by the boundary diffusion across the Ni_4W layer, there exists the following relationship between the exponents q and p [30].

$$q = \frac{1-p}{2} \tag{9}$$

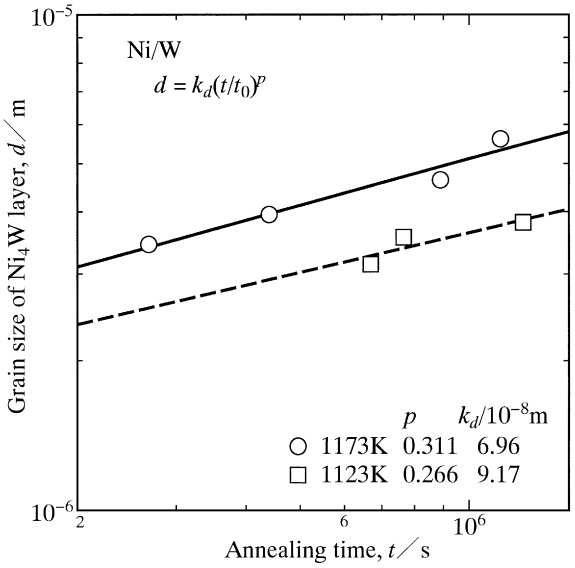

Fig. 5. The grain size d of the columnar grain in the Ni_4W layer versus the annealing time t shown as open squares and circles at 1123 K and 1173 K, respectively. Straight lines indicate the calculations from Eq. (8).

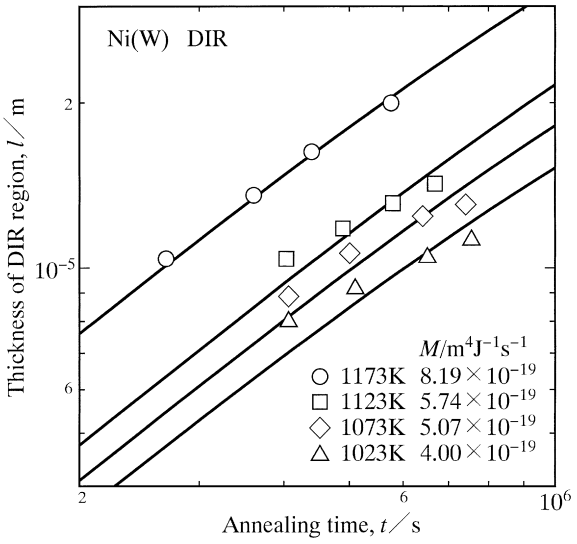

Fig. 6. The thickness l of the DIR region versus the annealing time t shown as open triangles, rhombuses, squares and circles at 1023 K, 1073 K, 1123 K and 1173 K, respectively. The results numerically calculated from Eqs. (11)–(17) are indicated as solid curves.

Using the mean values of p in Fig. 5, q was calculated from Eq. (9). The results of $T = 1123$ K and 1173 K are plotted as open squares in Fig. 4. At $T = 1173$ K, q is much smaller for the calculation than for the experiment, and the open square is located remarkably out of the error bars. This means that the contribution of boundary diffusion to the rate-controlling process is small and hence the growth of the Ni_4W layer is almost controlled by volume diffusion. On the other hand, at $T = 1123$ K, q is lightly smaller for the calculation than for the experiment but not so dissimilar in the calculation and the experiment. Thus, at $T = 1123$ K, the boundary diffusion considerably contributes to the rate-controlling process. Although the observation of grain growth could not be conducted at $T = 1023$–1073 K as mentioned earlier, the boundary diffusion contribution monotonically increases with decreasing annealing temperature [31]. Consequently, as shown in Fig. 4, the exponent q gradually decreases with decreasing annealing temperature T [28].

3.3. Growth behavior of DIR region

The microstructure observation in Section 3.1 indicates that the DIR region is formed at the Ni_4W/Ni interface and grows into the Ni specimen at $T = 1023$–1173 K. From the OM photographs like Fig. 1, the mean thickness l of the DIR region was determined by the following equation of the same formula as Eq. (3).

$$l = \frac{F}{w} \tag{10}$$

Here, F is the total area of the DIR region, and w is the total length of the DIR region parallel to the W/Ni_4W interface. The results of $T = 1023$ K, 1073 K, 1123 K and 1173 K are indicated as open triangles, rhombuses, squares and circles, respectively, in Fig. 6. In this figure, the ordinate and the abscissa show the logarithms of l and t, respectively. As can be seen, the thickness l monotonically increases with increasing annealing time t at each annealing temperature. The higher the annealing temperature is, the faster the DIR region grows. In a previous study [32], a new extended (NE) model was proposed to describe mathematically the growth rate of the DIR region in the A(B) system. Here, the notation A(B) indicates that a solute B diffuses into either a pure metal A or a binary A–B alloy of the A-rich single-phase according to convention. Furthermore, like Ni and W, elements A and B are nonvolatile at annealing temperatures. Thus, the NE model is applicable to DIR in the Ni(W) system. This model will be explained briefly below.

When one mol of the DIR region with composition y_e is produced from $(y_e - y_0)/(1 - y_0)$ mol of element B and $(1 - y_e)/(1 - y_0)$ mol of the A-rich solid-solution (α) phase with composition y_0, y_e is expressed as a function of l, s, r, δ, D^b and y_i by the following equation according to the NE model [32].

$$y_e = \frac{y_0 slr + y_i 2\delta D^b}{slr + 2\delta D^b} \tag{11}$$

Here, s is the diameter of the columnar grain in the DIR region, r is the migration rate of the moving boundary of the DIR region, D^b is the boundary diffusion coefficient of element B along the grain boundary in the DIR region, and δ is the thickness of the grain boundary. The temperature dependence of D^b is usually described by the following equation of the same formula as Eq. (2).

$$\sigma\delta D^b = \sigma\delta D_0^b \exp\left(-\frac{Q^b}{RT}\right) \tag{12}$$

Here, σ is the segregation factor of element B in the grain boundary, D_0^b is the pre-exponential factor, and Q^b is the activation enthalpy. The term $\sigma\delta D^b$ is hereafter called the boundary diffusivity. On the other hand, the migration rate r is related to the effective driving force $\Delta^{ef}G$ acting on the moving boundary by the equation

$$r = \frac{dl}{dt} = M\Delta^{ef}G, \tag{13}$$

where M is the mobility of the moving boundary. According to Eq. (13), the growth rate dl/dt of the DIR region is equal to r, and r is proportional to $\Delta^{ef}G$. Since $\Delta^{ef}G$ possesses the dimension of force per unit area or energy per unit volume, the dimension of M is m^4/J s on condition that l, t and $\Delta^{ef}G$ are measured in m, s and J/m^3, respectively. During growth of the DIR region, a penetration zone of element B is formed by volume diffusion in the untransformed matrix of the α phase ahead of the moving boundary. As a result, $\Delta^{ef}G$ is expressed by the following equation [32].

$$\Delta^{ef}G = (1 - y_e)\left\{\frac{RT}{V_m}\left(\ln\frac{1 - y_{nf}}{1 - y_e} + \frac{y_0}{1 - y_0}\ln\frac{y_{nf}}{y_e}\right) - Y\eta^2\frac{(y_{nf} - y_0)^2}{1 - y_0}\right\} \tag{14}$$

Here, y_{nf} is the composition of the penetration zone at the interatomic distance λ from the moving boundary, Y is the biaxial elastic

modulus of the untransformed matrix along the plane parallel to the moving boundary, and η is the misfit parameter. If the α phase is elastically isotropic, Y is described as

$$Y = \frac{E}{1-\nu}, \tag{15}$$

where E and ν are the Young's modulus and the Poisson's ratio, respectively. Let y_{pf} be the composition in the penetration zone at the interface between the untransformed matrix and the moving boundary. This interface is called the front interface. The composition y_{nf} in Eq. (14) is approximately expressed as a function of y_{pf}, y_0, r and λ by the equation [32]

$$y_{nf} = y_0 + (y_{pf} - y_0)\exp\left(-\frac{r\lambda}{D}\right), \tag{16}$$

where D is the diffusion coefficient for volume diffusion of element B in the penetration zone. Considering the local equilibrium between the moving boundary and the penetration zone at the front interface, y_{pf} is evaluated by the parallel-tangent construction (PTC) method [33]. When the concentration gradient of element B across the moving boundary is negligible, the following equation is obtained by the PTC method:

$$\ln\frac{y_{pf}}{1-y_{pf}} + \frac{2YV_m\eta^2}{RT}(y_{pf}-y_0) = \ln\frac{y_e}{1-y_e}. \tag{17}$$

As to the parameters in Eqs. (15)–(17), the following values were reported for the Ni(W) system: $E = 199.5$ GPa, $\nu = 0.312$ and $V_m = 6.5876\times10^{-6}$ m^3/mol [34]; $\eta = 0.126119$ [35]; and $\lambda = 0.3$ nm [32]. Since y is close to 0 in the penetration zone ahead of the moving boundary as shown in Fig. 2, D is almost equal to D^*_W [22,23]. Thus, the relationship between l and t is evaluated from Eqs. (11)–(17) on condition that $\sigma\delta D^b_0$ and Q^b in Eq. (12) are known. Unfortunately, however, reliable information on $\sigma\delta D^b_{W0}$ and Q^b_W is not available for the boundary diffusivity $\sigma\delta D^b_W$ of W in Ni.

The boundary diffusivity $\sigma\delta D^b_{Au}$ of Au in Ni was experimentally examined by Chatterjee and Fabian [36]. On the basis of their original result, $\sigma\delta D^b_{Au0}$ and Q^b_{Au} for $\sigma\delta D^b_{Au}$ were revaluated as 3.45×10^{-12} m^3/s and 167.7 kJ/mol, respectively, by Kaur et al. [37] On the other hand, Paul and Agarwala [38] experimentally determined $\sigma\delta D^b_{Nd0} = 3.50\times10^{-15}$ m^3/s and $Q^b_{Nd} = 119.6$ kJ/mol for the boundary diffusivity $\sigma\delta D^b_{Nd}$ of Nd in Ni. Since the atomic number is 60, 74 and 79 for Nd, W and Au, respectively, $\sigma\delta D^b_W$ may take an intermediate value between $\sigma\delta D^b_{Nd}$ and $\sigma\delta D^b_{Au}$. Consequently, $\sigma\delta D^b_{W0}$ and Q^b_W were estimated from $\sigma\delta D^b_{Nd0}$, $\sigma\delta D^b_{Au0}$, Q^b_{Nd} and Q^b_{Au} as follows

$$\sigma\delta D^b_{W0} = \sqrt{\sigma\delta D^b_{Nd0}\times\sigma\delta D^b_{Au0}} \tag{18a}$$

and

$$Q^b_W = \frac{Q^b_{Nd}+Q^b_{Au}}{2}. \tag{18b}$$

From Eq. (18a)–(18b), we obtain $\sigma\delta D^b_{W0} = 1.10\times10^{-13}$ m^3/s and $Q^b_W = 143.7$ kJ/mol. Unlike ordinary boundary diffusion, the segregation factor σ is not included in the kinetic formula of Eq. (11) for DIR [32]. Hence, the value of σ is necessary for conversion of $\sigma\delta D^b_W$ into δD^b_W. However, no reliable information is available for σ of W in Ni. Furthermore, there exists uncertainty in the estimation of $\sigma\delta D^b_{W0}$ and Q^b_W. Therefore, σ was assumed to be unity for the conversion.

Using $y_0 = 0$ as well as the parameters mentioned above, the thickness l_i was numerically calculated at each experimental annealing time t_i from Eqs. (11)–(17). For this calculation, y_i was considered equal to the solubility of W in Ni. Hence, $y_i = 0.126$, 0.127, 0.130 and 0.140 at $T = 1023$ K, 1073 K, 1123 K and 1173 K, respectively [5]. As shown in Fig. 1, the DIR region seems to be a polycrystalline mono-grain layer, and s and l are rather close to each other. Hence, for simplicity, it was assumed that $s = l$. As a result, the mobility M in Eq. (13) remains as the only unknown parameter. Unfortunately, however, no reliable information on M is available for DIR in the Ni(W) system. Thus, M was selected as the fitting parameter to minimize the function f defined as

$$f = \sum_{i=1}^{j}(l_i - l_i^e)^2. \tag{19}$$

Here, l_i^e is the experimental value of l at $t = t_i$, and $j = 4$ at $T = 1023$–1173 K. The estimated values of M are shown in Fig. 6. Using these values of M, l was calculated as a function of t from Eqs. (11)–(17). The results of $T = 1023$–1173 K are shown as solid curves in Fig. 6. Although the plotted points are slightly scattered from each solid curve at $T = 1023$–1123 K, the dependence of l on t is satisfactorily reproduced by the calculation. Particularly at $T = 1173$ K, the calculation well coincides with the experiment.

The calculation with Eqs. (11)–(17) was carried out up to $t = 10^8$ s to evaluate the growth behavior of the DIR region across a wide range of annealing time. The value $t = 10^8$ s is more than two orders of magnitude greater than the longest annealing time at each annealing temperature. The results of $T = 1023$ K, 1073 K, 1123 K and 1173 K are shown as solid curves in Fig. 7(a–d), respectively. In this figure, like Fig. 6, the ordinate and the abscissa indicate the logarithms of l and t, respectively. Furthermore, the open triangles, rhombuses, squares and circles in Fig. 6 are represented as open circles in Fig. 7(a–d), respectively. The thickness l of the DIR region may be described as a power function of the annealing time t by the following equation of the same formula as Eqs. (4) and (8):

$$l = k\left(\frac{t}{t_0}\right)^n, \tag{20}$$

where k is the proportionality coefficient with the same dimension as l and n is the exponent. If the growth of the DIR region is controlled by the interface reaction at the moving boundary, l is proportional to t and thus n is equal to unity [32]. This is just the case in the early stages of the reaction in Fig. 7. Inserting $n = 1$ into Eq. (20), we obtain the following equation for this type of rate-controlling process.

$$l = \frac{k}{t_0}t = Kt \tag{21}$$

Here, K is the kinetic coefficient with a dimension of m/s. From the solid curves in Fig. 7, $K = 1.81\times10^{-11}$ m/s, 2.07×10^{-11} m/s, 2.39×10^{-11} m/s and 3.85×10^{-11} m/s are obtained at $T = 1023$ K, 1073 K, 1123 K and 1173 K, respectively. On the other hand, n gradually decreases with increasing annealing time t and then reaches to constant values of 0.469, 0.472, 0.475 and 0.468 in the late stages of the reaction at $T = 1023$ K, 1073 K, 1123 K and 1173 K, respectively. In the early stages, the thickness l is very small, and hence an abundant amount of the solute can be transported by the boundary diffusion across the DIR region. In such a case, the interface reaction at the moving boundary becomes the bottleneck for the growth of the DIR region. On the other hand, in the late stages, l is very large, and thus the solute has to be transported by the boundary diffusion over long distances across the DIR region. As a result, the boundary diffusion governs the rate-controlling process, but the interface reaction is no longer the bottleneck. Consequently, the growth of the DIR region is controlled by the interface reaction in the early stages but by the boundary diffusion in the late stages [32]. For each solid curve in Fig. 7, the extrapolation is indicated as dashed lines in the early and late stages of the reaction. As can be seen, most of the open circles are located in the intermediate stages of the reaction. Thus, it is concluded that the interface reaction as well as the

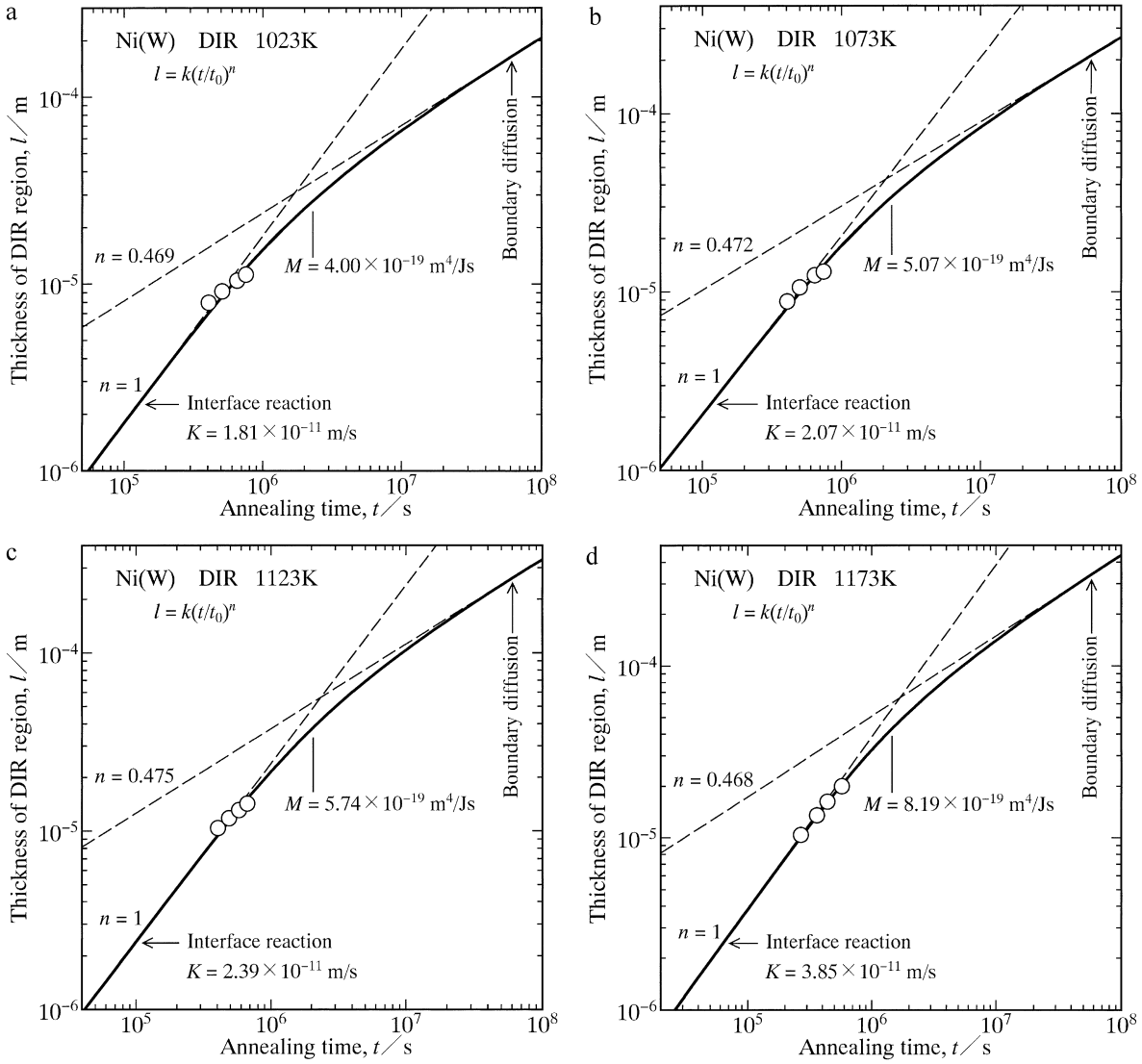

Fig. 7. The annealing time dependencies of the thickness l of the DIR region numerically calculated from Eqs. (11)–(17) at (a) 1023 K, (b) 1073 K, (c) 1123 K and (d) 1173 K are shown as solid curves. The experimental result in Fig. 6 is indicated again as open circles at each annealing temperature. The solid curve is extrapolated as dashed lines in the early and late stages of the reaction.

boundary diffusion contributes to the growth of the DIR region at the experimental annealing times.

As stated above, M was chosen as the fitting parameter to calculate the model curves in Fig. 6. The values of M are plotted as open circles against the annealing temperature T in Fig. 8. In this figure, the ordinate shows the logarithm of M, and the abscissa indicates the reciprocal of T. As can be seen, the open circles lie well on a straight line. This means that the temperature dependence of M is expressed by the following equation of the same formula as Eqs. (2) and (12):

$$M = M_0 \exp\left(-\frac{Q_M}{RT}\right). \tag{22}$$

From the open circles in Fig. 8, the pre-exponential factor and the activation enthalpy in Eq. (22) were determined to be $M_0 = 7.84 \times 10^{-17}$ m^4/J s and $Q_M = 45.1$ kJ/mol, respectively, by the least-squares method as shown with a solid line. In the early stages of the reaction, the thickness l is proportional to the annealing time t according to Eq. (21). In a manner similar to Fig. 8, the values of K are plotted as open circles against the annealing temperature T in Fig. 9. In this figure, the ordinate shows the logarithm of K, and the abscissa indicates the reciprocal of T. Although the open circles are slightly scattered, the temperature dependence of K may be expressed by the following equation.

$$K = K_0 \exp\left(-\frac{Q_K}{RT}\right) \tag{23}$$

Here, $K_0 = 4.51 \times 10^{-9}$ m/s and $Q_K = 47.6$ kJ/mol. Thus, Q_K is close to $Q_M = 45.1$ kJ/mol but much smaller than $Q^b = 143.7$ kJ/mol. The activation enthalpy for the boundary diffusion along the grain boundary may not be so different from that for the boundary diffusion across the grain boundary. Hence, the difference between Q_M and Q^b indicates that the boundary diffusion across the moving boundary does not necessarily correspond to the predominant process of the interface reaction for DIR in the Ni(W) system. On the other hand, we obtain the relationship $K = M\Delta^{ef}G$ from Eqs. (13) and (21). According to this relationship, the similarity in Q_K and Q_M implies that the dependence of $\Delta^{ef}G$ on T in the early stages is rather small in the temperature range of $T = 1023$–1173 K.

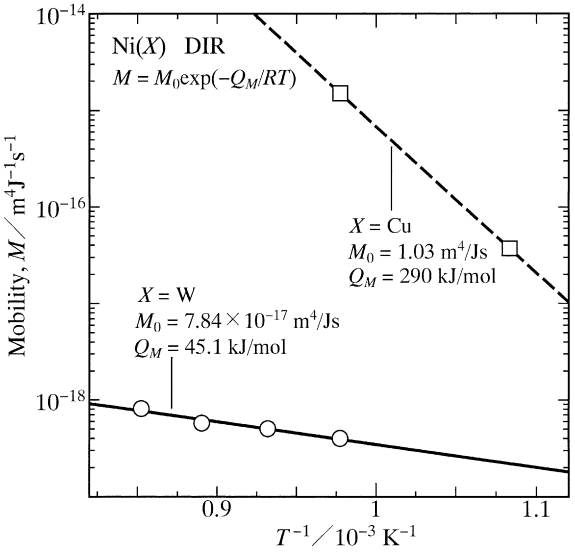

Fig. 8. The mobility M for the moving boundary of the DIR region versus the reciprocal of the annealing temperature T shown as open circles. A solid line indicates the calculation from Eq. (22). The corresponding result of DIR in the Ni(Cu) system in a previous study [32] is represented as open squares with a dashed line.

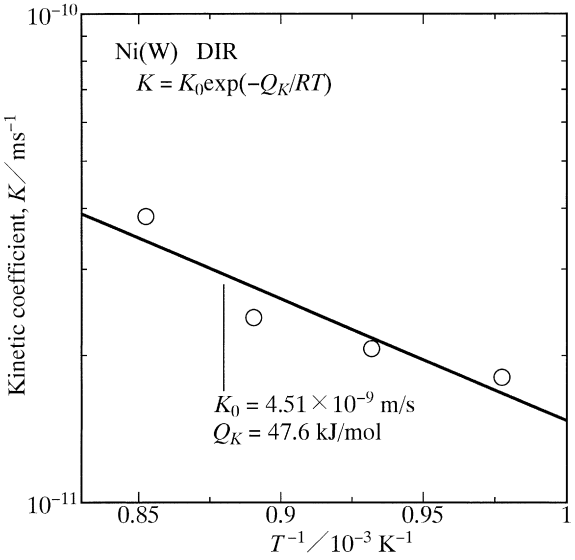

Fig. 9. The kinetic coefficient K versus the reciprocal of the annealing temperature T shown as open circles. A solid line indicates the calculation from Eq. (23).

The values of M for DIR in the Ni(Cu) system reported in a previous study [32] are represented as open squares with a dashed line of $M_0 = 1.03\ \mathrm{m^4/J\,s}$ and $Q_M = 290$ kJ/mol in Fig. 8. As can be seen, the absolute value of M as well as the activation enthalpy Q_M is much smaller for the Ni(W) system than for the Ni(Cu) system. As previously mentioned, $\sigma\delta D^{b}_{W}$ was estimated from $\sigma\delta D^{b}_{Nd}$ and $\sigma\delta D^{b}_{Au}$ by Eq. (18a) and (18b). Therefore, there will exist uncertainty in the estimation. As a consequence, the comparison of M between the Ni(W) and Ni(Cu) systems possesses less physical meaning so far. In order to improve the reliability of M for DIR in the Ni(W) system, experimental information on the boundary diffusion of W in Ni is essentially important.

4. Conclusions

The solid-state reactive diffusion between Ni and W was experimentally examined using the Ni/W/Ni diffusion couple in the temperature range between $T = 1023$ K and 1173 K. During annealing, the Ni_4W layer is formed at the Ni/W interface in the diffusion couple and grows mostly towards the Ni specimen. The growth of the Ni_4W layer is controlled mainly by volume diffusion at $T = 1173$ K but by boundary and volume diffusion at $T < 1173$ K. The contribution of boundary diffusion to the rate-controlling process increases with decreasing annealing temperature. Furthermore, the DIR region alloyed with W is produced at the Ni_4W/Ni interface and grows into the Ni specimen. The concentration of W in the DIR region at the Ni_4W/Ni interface coincides with the solubility of W in Ni. Thus, the local equilibrium is realized at the Ni_4W/Ni interface. The growth behavior of the DIR region was numerically analyzed using the new extended-model proposed in a previous study [32]. The analysis indicates that the thickness l of the DIR region is proportional to the annealing time t in the early stages of the reaction but to a power function of t in the late stages of the reaction. Here, the exponent of the power function is smaller than 0.5. Thus, the growth of the DIR region is controlled by the interface reaction at the moving boundary in the early stages but by the boundary diffusion across the DIR region in the late stages. Since most of the experimental annealing times are located in the intermediate stages of the reaction, the interface reaction as well as the boundary diffusion contributes to the rate controlling process of DIR under the present experimental conditions.

Acknowledgements

The present study was supported by the Iketani Science and Technology Foundation in Japan. The study was also partially supported by a Grant-in-Aid for Scientific Research from the Ministry of Education, Culture, Sports, Science and Technology of Japan.

References

[1] Y. Xu, F.C. Laabs, B.J. Beaudry, K.A. Gschneidner, J. Appl. Phys. 69 (1991) 4292.
[2] I.S. Batra, G.B. Kale, T.K. Saha, A.K. Ray, J. Derose, J. Krishnan, Mater. Sci. Eng. A 369 (2004) 119.
[3] Z. Zhong, T. Hinoki, A. Kohyama, Mater. Sci. Eng. A 518 (2009) 167.
[4] Z. Zhong, T. Hinoki, H.-C. Jung, Y.-H. Park, A. Kohyama, Mater. Des. 31 (2010) 1070.
[5] T.B. Massalski, H. Okamoto, P.R. Subramanian, L. Kacprzak, Binary Alloy Phase Diagrams, vol. 3, ASM International, Materials Park, OH, 1990, p. 2883.
[6] Metals Data Book, ed. by Japan Inst. Met., Maruzen, Tokyo, (2000) pp. 21–23.
[7] Y. Muranishi, M. Kajihara, Mater. Sci. Eng. A 404 (2005) 33.
[8] M. Kajihara, T. Yamada, K. Miura, N. Kurokawa, K. Sakamoto, Netsushori 43 (2003) 297.
[9] T. Yamada, K. Miura, M. Kajihara, N. Kurokawa, K. Sakamoto, J. Mater. Sci. 39 (2004) 2327.
[10] T. Yamada, K. Miura, M. Kajihara, N. Kurokawa, K. Sakamoto, Mater. Sci. Eng. A 390 (2005) 118.
[11] M. Kajihara, T. Takenaka, Mater. Sci. Forum 539–543 (2007) 2473.
[12] T.B. Massalski, H. Okamoto, P.R. Subramanian, L. Kacprzak, Binary Alloy Phase Diagrams, vol. 1, ASM International, Materials Park, OH, 1990, p. 434.
[13] M. Kajihara, Acta Mater. 52 (2004) 1193.
[14] J.M. Walsh, M.J. Donachie Jr., Metall. Trans. 4 (1973) 2854.
[15] K.E. Poulsen, S. Rubaek, E.W. Langer, Scripta Metall. 8 (1974) 1297.
[16] R. Cury, J.-M. Joubert, S. Tusseau-Nenez, E. Leroy, A. Allavena-Valette, Intermetallics 17 (2009) 174.
[17] F.J.A. den Broeder, S. Nakahara, Scripta Metall. 17 (1983) 399.
[18] D. Liu, W.A. Miller, K.T. Aust, Acta Metall. 37 (1989) 3367.
[19] C.Y. Ma, E. Rabkin, W. Gust, S.E. Hsu, Acta Metall. Mater. 43 (1995) 3113.
[20] P.G. Shewmon, Diffusion in Solids, McGraw-Hill, New York, 1963, p. 14.
[21] M.S.A. Karunaratne, P. Carter, R.C. Reed, Mater. Sci. Eng. A 281 (2000) 229.
[22] G.S. Hartley, Trans. Faraday Soc. 27 (1931) 10.
[23] L.S. Darken, Trans. AIME 175 (1948) 184.
[24] M. Kajihara, Mater. Sci. Eng. A 403 (2005) 234.
[25] M. Kajihara, Defect Diffus. Forum 249 (2006) 91.
[26] M. Kajihara, Mater. Trans. 46 (2005) 2142.
[27] M. Kajihara, Mater. Trans. 47 (2006) 1480.
[28] A. Furuto, M. Kajihara, Mater. Trans. 49 (2008) 294.
[29] T. Takenaka, M. Kajihara, N. Kurokawa, K. Sakamoto, Mater. Sci. Eng. A 406 (2005) 134.
[30] Y.L. Corcoran, A.H. King, N. de Lanerolle, B. Kim, J. Electron. Mater. 19 (1990) 1177.

[31] T. Takenaka, S. Kano, M. Kajihara, N. Kurokawa, K. Sakamoto, Mater. Sci. Eng. A 396 (2005) 115.
[32] Y. Yamamoto, M. Kajihara, Mater. Trans. 42 (2001) 1763.
[33] M. Hillert, in: H.I. Aaronson (Ed.), Lectures on the Theory of Phase Transformations, 2nd edition, TMS-AIME, Warrendale, PA, 1999, p. 1.
[34] S. Nishikawa, Introduction to Metallurgy, AGNE, Tokyo, 2001, p. 530.
[35] Y. Mishima, S. Ochiai, T. Suzuki, Acta Metall. 33 (1985) 1161.
[36] A. Chatterjee, D.J. Fabian, J. Inst. Met. 96 (1968) 186.
[37] I. Kaur, W. Gust, L. Kozma, Handbook of Grain and Interphase Boundary Diffusion Data, vol. 2, Ziegler Press, Stuttgart, 1989, p. 992.
[38] A.R. Paul, R.P. Agarwala, Metall. Trans. 2 (1971) 2691.